Published in final edited form as:
Nat Chem Biol. 2017 September ; 13(9): 956–960. doi:10.1038/nchembio.2428.

The structure of vanadium nitrogenase reveals an unusual bridging ligand

Daniel Sippel and **Oliver Einsle***
Lehrstuhl Biochemie, Institut für Biochemie, Albert-Ludwigs-Universität Freiburg, Albertstrasse 21, 79104 Freiburg, Germany, Freiburg Research Institute for Advanced Studies (FRIAS), Albertstrasse 19, 79104 Freiburg, Germany, and BIOSS Centre for Biological Signalling Studies, Schänzlestrasse 1, 79104 Freiburg, Germany

Abstract

Nitrogenases catalyze the reduction of N_2 gas to ammonium at a complex heterometallic cofactor. Most commonly this is the FeMo cofactor (FeMoco), a [Mo:7Fe:9S:C] cluster whose exact reactivity and substrate binding mode remain unknown. Alternative nitrogenases replace molybdenum with either vanadium or iron and differ in reactivity, prominently in the ability of vanadium nitrogenase to reduce CO to hydrocarbons. Here we report the 1.35 Å structure of vanadium nitrogenase from *Azotobacter vinelandii*. The 240 kDa protein contains an additional α-helical subunit not present in molybdenum nitrogenase. The FeV cofactor (FeVco) is a [V:7Fe:8S:C] cluster with a homocitrate ligand to vanadium. Unexpectedly, it lacks one sulfide ion compared to FeMoco that is replaced by a bridging ligand, likely a μ-1,3-carbonate. The anion fits into a pocket within the protein that is obstructed in molybdenum nitrogenase, and its different chemical character helps to rationalize the altered chemical properties of this unique N_2- and CO-fixing enzyme.

Introduction

Nitrogenase is the only biological catalyst for the reductive fixation of atmospheric dinitrogen (N_2) into bioavailable ammonium (NH_4^+). Its reaction is equivalent to the industrial Haber-Bosch process, but its extraordinary ability to break the stable N_2 triple bond at ambient temperature and pressure is unmatched.[1,2] Nitrogenase is a two-component complex that drives catalysis with low-potential electrons from central metabolism, supported by extensive ATP hydrolysis.[3,4] Electrons are delivered to a [4Fe:4S] cluster in the Fe protein component that then binds ATP and consequently associates with the N_2-

Correspondence and requests for materials should be addressed to O.E. (einsle@biochemie.uni-freiburg.de).

Author Contributions D.S. performed the experiments and built and refined the structural model, O.E. designed the experiments, built and refined the structural model, and wrote the manuscript.

Author Information The authors declare no competing financial interests.

Data Availability
The structural model and structure factors have been deposited with the Protein Data Bank with accession code 5N6Y. All other data supporting the findings of this study are contained in the published article (and its supplementary information files) or are available from the corresponding author upon reasonable request.

Europe PMC Funders Author Manuscripts

reducing component. The Fe protein then hydrolyzes ATP and transfers an electron *via* an [8Fe:7S] relay, the P-cluster, to a complex active site cofactor where substrate reduction takes place. Known nitrogenases share a single evolutionary origin, and it is primarily the chemical nature of this cofactor that defines three classes, the Mo-, V- and Fe-dependent nitrogenases.5 Most organisms employ a heterometallic cluster containing iron and molybdenum, the FeMo cofactor (FeMoco). This [Mo:7Fe:9S:C] moiety includes a homocitrate ligand to molybdenum, and understanding its structure and functionality has been an ongoing challenge for decades.6

Early studies on *A. vinelandii* indicated that Mo was not essential for nitrogen fixation in this organism,7 and deletion strains lacking the structural genes for molybdenum nitrogenase (Δ*nifHDK*) retained the capacity for diazotrophic growth.8,9 The alternative nitrogenase of *Azotobacter chroococcum* requires vanadium,10 and isolation of a vanadium nitrogenase was reported shortly thereafter from *A. vinelandii* 11 and *A. chroococcum*.12 The *vnf* gene cluster for vanadium nitrogenase of *A. vinelandii* includes a distinct Fe protein (VnfH) and a catalytic VFe protein that contains an additional subunit, encoded by the *vnfG* gene.13 During ATP-dependent N_2 fixation, vanadium nitrogenase diverts a larger portion of the electron flux from Fe protein towards H_2 formation than molybdenum nitrogenase. This can lead to the VFe protein acting purely as a hydrogenase, but even under high pN_2, the minimum observed reaction stoichiometry is

$$N_2 + 12e^- + 14H^+ + 40\,MgATP \rightarrow 2NH_4^+ + 3H_2 + 40\,MgADP + 40\,P_i$$

for the *A. chroococcum* enzyme,14 as compared to only 1 H_2 per N_2 for molybdenum nitrogenase, at an expense of 16 MgATP. The specific activity of the *A. vinelandii* VFe protein is approximately 40 % of that of the MoFe protein.11,15,16

Unexpectedly, vanadium nitrogenase also reduces carbon monoxide (CO), a non-competitive inhibitor for all known substrates other than protons.17 CO is isoelectronic to N_2, and non-competitive inhibition must not rule out a similar mode of binding to the cofactor, as CO can bind to a less-reduced state of the cluster where N_2 binding will not occur. In contrast to the chemically comparable Fischer-Tropsch process,18 CO reduction by VFe protein does not proceed quantitatively to methane, CH_4. It yields a variety of partially unsaturated hydrocarbon products with carbon chain lengths of 2–7,19 raising an interest in biological hydrocarbon formation for energy conservation.20 Spectroscopic studies with CO and molybdenum nitrogenase indicated that a complex is formed under turnover conditions, 21,22 and its recent isolation and rapid crystallization represented the first structure of a ligand-bound state of FeMoco, where CO reversibly replaced a belt sulfide of the cofactor, leading to a μ_2-carbonyl adduct bridging irons Fe2 and Fe6.23 The belt sulfide can also be replaced by selenide, Se^{2-}, suggesting structural flexibility around the cofactor belt.24

The CO-reducing activity of the VFe protein exceeds that of the MoFe protein by a factor of 800, highlighting the functional differences between FeMoco and the corresponding FeVco. 5 Spectroscopic data points towards structural analogy of both cofactors, but the differences in reactivity cannot be straightforwardly rationalized without detailed structural information. Mo availability regulates the induction of the V-dependent alternative,10 and while earlier

studies largely relied on the aforementioned Δ*nifHDK* strain,8,9 later also in a histidine-tagged version,15 we recently established the preparation of VFe protein from unmodified, nitrogen-fixing *A. vinelandii* through depletion of Mo in the growth medium.25 We have produced VFe protein from the *A. vinelandii* type strain growing diazotrophically, with N_2 as the sole nitrogen source, and isolated the enzyme under strict exclusion of dioxygen. Here, we have grown high-quality single crystals that allowed us to solve the structure of vanadium nitrogenase, including FeVco, by X-ray diffraction analysis.

Results

Overall architecture of vanadium nitrogenase

Crystals of *A. vinelandii* vanadium nitrogenase belonged to space group *P*1 and diffracted to 1.35 Å resolution using synchrotron radiation. The structure was solved by multiple-wavelength anomalous dispersion and established that VFe protein is a $VnfD_2K_2G_2$ complex (Fig. 1a). The peptide chains of the three gene products were almost completely defined in the electron density map, with the model comprising residues 2–474 of VnfD, 12–475 of VnfK and 2–113 of VnfG (Supplementary Results, Supplementary Fig. 1). The core of the enzyme, a dimer of VnfDK heterodimers, corresponds to the $NifD_2K_2$ arrangement of the MoFe protein and aligned to it with a root-mean-squared deviation of 1.97 Å for all atoms (Fig, 1b,c and Supplementary Fig. 2). These subunits were composed of three consecutive Rossmann fold domains, hinting towards early gene duplication events during the genesis of a nitrogenase ancestor. In the MoFe protein, NifK contains an extended N terminus of approximately 50 residues that wraps around the neighboring NifD, stabilizing the heterodimer. This extension was absent in VnfK, replaced by an additional β-strand (residues 13–18) that complemented the parallel β-sheet of the third domain of the subunit.

The metal clusters retained their position in the paralog, with the P-cluster residing in the VnfD/K interface, while the FeV cofactor was cradled within the VnfD subunit. In the MoFe protein, an additional metal site was assigned as a Ca^{2+} ion26 that under given conditions can be replaced by an additional iron.27 In *A. vinelandii* VFe protein, the same binding site is occupied by Mg^{2+}, as evidenced by the bond distances and coordination geometry of the ion (Supplementary Fig. 3). The cation strengthens the interaction between the two VnfK subunits in the enzyme, while VnfD is only peripherally involved by providing two lysine residues to the second coordination sphere (Supplementary Fig. 3). The additional subunit of the VFe protein, VnfG, is a globular 113 amino acid polypeptide arranged into four α-helices that exclusively contacts VnfD, but not VnfK (Fig. 1d). The importance of VnfG for the reactivity of the VFe protein remains unclear, but an involvement in transferring FeV cofactor to the apoenzyme has been suggested, based on similarity to the proposed cofactor chaperones NafY from *A. vinelandii*28 and NifY of *K. pneumoniae*.29 In this scenario, VnfG may guide the mature cofactor to an apo-$VnfD_2K_2$ heterotetramer that is in an open conformation as seen in apo-$NifD_2K_2$ obtained from a Δ*nifB* strain,30 and subsequently remain bound as a constituent subunit of the enzyme. In the structure, VnfG is in close contact with the presumed insertion site for the cofactor into VFe protein at the third domain of VnfD (Fig. 1a, b). However, VnfG does not exhibit structural homologies with either the N-terminal or the core domain of the NafY protein implicated in cofactor delivery.28,31 A

possible interference of VnfG with the binding of the Fe protein, $VnfH_2$, during catalysis has been discussed,15 but as this docking site is likely retained at the VnfDK interface, the observed binding of VnfG is sufficiently remote not to interfere with the formation of a complex analogous to the one observed for molybdenum nitrogenase, even considering the variations seen in different nucleotide-bound or -free states (Supplementary Fig. 4).32,33

An [8Fe:7S] P-cluster in a redox equilibrium

Although a structural difference between the P-clusters of MoFe and VFe protein was previously suggested,15 most studies highlighted the similar properties of the electron relays that include conservation of all six cysteine ligands.14 In the VFe protein, the P-cluster is an [8Fe:7S] moiety that retains the unique topology of its counterpart in the MoFe protein. In its dithionite-reduced P^N state it resembles two canonical [4Fe:4S] clusters fused *via* a shared sulfide ion (Fig. 2a,b). It resides on the twofold pseudosymmetry axis relating VnfD and VnfK (Fig. 2c) and is coordinated by residues C49, C75 and C138 from VnfD, as well as C31, C56 and C115 from VnfK. Upon oxidation, the P-cluster of the MoFe protein undergoes a conformational change of two Fe ions, Fe5 and Fe6, leading to the two-electron oxidized P^{Ox} state.34 In the VFe protein, we observed a mixed redox state in electron density maps (Fig. 2b), as frequently observed in crystal structure analyses. Here, however, only Fe6 changed its position and broke its coordinative bond to the central sulfide S1 in favor of a new interaction with the harder ligand S153 in VnfK. By inference, the movement of only one Fe in the VFe protein might indicate that the cluster is oxidized only by one electron, which is in line with spectroscopic data:35 As the P^N state of the cluster likely is the same diamagnetic all-ferrous species as in MoFe protein, the Fe6-oxidized center should then represent a P^{+1} site.

Structure of the FeV cofactor

The catalytic FeV cofactor is nested within the three domains of the VnfD subunit. Like its counterpart in molybdenum nitrogenase it is linked to the protein only *via* two coordinative interactions, from Fe1 to C257 and from V to H423. A further, bidentate ligand to V is an organic homocitrate moiety, coordinating the metal in a mode and geometry that is virtually identical to the one observed in the MoFe protein. At 1.35 Å resolution the central carbide can be unambiguously assigned, confirming its previous detection by X-ray emission spectroscopy (Fig. 3a and Supplementary Fig. 5a,b).36 Interestingly, the exchange of Mo in FeMoco for V in FeVco implies only minimal changes of geometry and bond distances (Fig. 3b). With an octahedral ligand environment, the adjacent sulfides of the cofactor refined to distances of 2.36 Å (S1B), 2.37 Å (S3B) and 2.32 Å (S4B), almost indistinguishable from the corresponding distances in the structure of FeMoco – 2.36 Å, 2.37 Å and 2.35 Å, respectively – that was determined at 1.0 Å resolution.37 On the other hand, the V–Fe distances in FeVco are slightly longer than in FeMoco, averaging 2.77 Å *vs.* 2.69 Å, respectively, reflecting observations made in cubane model complexes.38 Consequently, the overall geometry of the FeV cofactor is slightly elongated, but otherwise very similar to the FeMo cofactor.

A major difference between the two clusters, however, is the replacement of one belt sulfide (S3A) that in FeMoco links Fe4 and Fe5, by a second ligand that coordinates both irons in a

μ-bridging fashion. It extends the Fe4–Fe5 distance from 2.61 Å in FeMoco to 2.76 Å in FeVco, in turn contributing to shortening the V–Fe5 distance (Fig. 3a,c). This ligand is a *C*3-symmetric tetraatomic molecule that is very well-defined in the electron density maps (Supplementary Fig. 5), with all bond distances refining to values of 1.27–1.3 Å. The electron density feature is fully explained with a carbonate ligand, CO_3^{2-}, or with the isoelectronic nitrate, NO_3^- (Supplementary Fig. 6a). An analysis of the electron density features that had been key to identifying the central light atom of FeMoco as a carbide37 indicated that the three outer atoms are oxygen, but was inconclusive for the central atom at this resolution (Supplementary Fig. 6b). As VFe protein was isolated from *A. vinelandii* cells growing diazotrophically, we tentatively assigned the ligand as carbonate, whose twofold negative charge is also in better agreement with the displaced S^{2-} than NO_3^-. Also, the presence of nitrate, as a nitrogen source, would effectively prevent further expression of nitrogenase and inhibit the activity of any nitrogenase already present through an ammonium-dependent switch-off. Other ligands that could alternatively be envisioned at this position are bicarbonate (HCO_3^-), acetate ($H_3C\text{-}COO^-$), and carbamate ($H_2N\text{-}COO^-$) (Supplementary Fig. 6a). In all cases, however, the bond distances should include a longer single bond that is not in agreement with the observed electron density (Supplementary Fig. 5b).

The ligand is slightly kinked on the Fe4–Fe5 edge of FeVco, with its molecular plane not entirely parallel to the *C*3-pseudosymmetry axis of the cofactor (Fig. 3c and Supplementary Fig. 5c). CO_3^{2-} is tightly cradled in a binding pocket in VnfD that is formed by a single loop of the protein chain, ^{335}TGGPRL^{340}, connecting beta strand β1 to helix α1 of the third domain of VnfD (Fig. 4a). The carbonate oxygen embedded in this loop forms three H-bonds, two of which link to the backbone amide nitrogens of G337 and R339, and the third to the hydroxyl group of T335. This coordination not only further excludes acetate as a ligand, but also carbamate, as G335 and R339 can act exclusively as H-bond donors. The question arises whether a similar exchange of a belt sulfide could possibly occur in FeMoco, especially as such a replacement with CO or Se^{2-} was demonstrated.23,24 In the MoFe protein, the corresponding loop region in vicinity to S3A is ^{355}IGGLRP^{360} of NifD. While similar in location and conformation, this loop has the positions of leucine and proline exchanged (Fig. 4b), so that residue P360 of NifD constricts the pocket, excluding the binding of a CO_3^{2-} ligand. It is thus the difference in protein sequence – and here the simple swap of two amino acids – that opens a pocket for a carbonate in the VFe protein, but not in the MoFe protein. Note that in FeMoco atom S3B acts as an acceptor for three hydrogen bonds from G356, G357 and R359 in the binding loop and thus is also very tightly held within the protein.

Discussion

The unprecedented ligand to FeVco, accommodated through the leucine–proline swap in the sequence of VnfD, will substantially influence cluster reactivity. An exchange of the single, bridging weak-field ligand sulfide for the harder carbonate oxygens not only leads to an extension of the cluster, but also to perturbations of the overall electronic structure that alter its catalytic properties. Although the complexes of MoFe protein with CO and Se^{2-} have established that an exchange of sulfide is possible, a recent theoretical study based on

electrostatic calculations pointed out that the removal of a sulfide in the form of H_2S is not facile and might represent the most energetically challenging step during catalysis.39

Hints toward the mechanisms of sulfide removal and carbonate insertion into FeVco arise from analysis of the *vnf* gene cluster of *A. vinelandii*.40 This cluster is a single locus on the *A. vinelandii* chromosome, presumably consisting of five operons with 17 open reading frames (Supplementary Fig. 7). Beside the structural genes for VFe protein and its corresponding Fe protein VnfH, the cluster contains distinct copies of the E, N and X genes likely responsible for vanadium insertion into the cofactor, the putative cofactor chaperone gene *vnfY* and the regulatory *vnfU* and *vnfA* genes. At least six additional open reading frames have no correspondence in the *nif* cluster. Three of these show homology to enzymes from the biogenesis of the cofactor molybdopterin that is utilized in molybdenum- and tungsten-containing proteins other than nitrogenase.41 Their presence in a cluster that is induced upon molybdenum starvation is puzzling at first, but the roles of the encoded proteins, homologs of MoeB, HesA and MoaD that we designate VnfP1, VnfP2 and VnfP3, might provide valuable clues. In molybdopterin biosynthesis, MoeB or HesA activate the terminal carboxylate of MoaD by adenylylation. MoaD is characterized by a C-terminal GG motif that is coupled to adenylate in a process related to ubiquitin activation by E1 enzymes.42 The MoeB–MoaD complex then receives sulfide from an unknown transferase to generate a terminal thiocarboxylate, from which the sulfide is passed to the cofactor precursor cyclic pyranopterin monophosphate (cPMP).41 The analogous system in the *vnf* cluster may not actually donate sulfide, but rather extract it from the cofactor precursor. The *vnf* cluster lacks a separate homolog of NifB, whose product, a topologically complete [8Fe:9S:C] cluster, thus must be the precursor for both FeMoco and FeVco.43 A means to extract belt sulfide S3A is thus required before carbonate binds, and VnfP1–3 may fulfil this role. VnfP1 would form a complex with the ubiquitin-like VnfP3, adenylylating its C-terminal glycine; the sulfur source for the formation of a thiocarboxylate might then be the cofactor precursor itself. Note that VnfP1 and VnfP2 share 32% sequence identity and may both be able to form a complex with VnfP3. However, VnfP2 lacks all the residues directly involved in ATP binding in the structure of *E. coli* MoeB,42 and it might thus interact more directly with the FeVco precursor in complex with VnfP3. Carbonate acts as a bridging carboxylate that may have been achieved more easily by a single point mutation introducing an Asp or Glu residue near the cofactor. However, this would have necessitated removal of S3A from the stable cofactor core *in situ*. We hypothesize that the machinery described above instead exchanges S3A for carbonate before the cofactor is inserted into VFe protein. Once in place and tightly coordinated, no further exchange of the carbonate ligand is possible.

Carbonate coordination in FeVco is reminiscent of μ-carboxylate-bridged diiron enzymes such as hemerythrin or methane monooxygenase that bind or activate O_2,44 although the rigid geometry of the nitrogenase cofactors results in a shorter Fe–Fe distance. With the structure of the VFe protein, attention is once more called to the unique belt sulfides of the nitrogenase cofactors. The first structure of a nitrogenase enzyme in a non-resting state was that of the MoFe protein with CO replacing S2B.23 Although CO is a non-competitive inhibitor of N_2 reduction and consequently should bind to a different site (or state) than the substrate itself, this work provided a glimpse of flexibility within the otherwise highly stable and rigid cofactor. The present finding of carbonate replacing a sulfide is in line with this,

although it is a different sulfide – S3A rather than S2B – that is exchanged. In the VFe protein, S2B bridges Fe2 and Fe6, and we explicitly do not imply that the location of carbonate highlights an actual substrate binding site. Its influence on the overall reactivity of the cluster, however, may explain the observed differences between FeMoco and FeVco. The structure of vanadium nitrogenase once more exemplifies the intricate fine-tuning of inorganic metal sites in biological systems that can inspire synthetic chemistry, and the particular reactivity of the VFe protein may open routes towards the future characterization of new substrate-bound states of the enzyme.

Online Methods

Growth of *A. vinelandii* and isolation of vanadium nitrogenase

Pure and unmodified vanadium nitrogenase VFe protein was produced as described elsewhere.25 In short, cells of *A. vinelandii* type strain were cultivated in molybdenum-free medium supplemented with Na_3VO_4 in the absence of a nitrogen source other than atmospheric N_2. Cells were singled out on agar plates for re-inoculation of Mo-free medium from a single colony and this process was repeated for five times. For cell production, a 100 mL pre-culture of Mo-free Burke's medium was inoculated with a single colony and grown overnight to then inoculate nitrogen-free main cultures of 500 mL. Cells were harvested by centrifugation at an optical density of 2–4 at 600 nm after approximately 18 h of aerobic growth. All following steps were carried out under strict exclusion of oxygen using modified Schlenk techniques or inert gas chambers. After cell lysis, the crude extract was subjected to two consecutive steps of anion exchange chromatography on HiTrap Q HP and Resource Q, respectively (GE Healthcare), followed by a final size-exclusion step on Superdex 200 (GE Healthcare). Pure VFe protein was concentrated to 30 $mg \cdot mL^{-1}$ and shock-frozen in liquid N_2 for further use.

Crystallization and data collection

A. vinelandii VFe protein was crystallized by sitting drop vapor diffusion under the strict exclusion of dioxygen in an inert gas chamber containing a 95/5 % mixture of N_2/H_2 with < 1 ppm of O_2. 1 μl of protein solution (5 $mg \cdot mL^{-1}$) was mixed with the same volume of a reservoir solution containing 10–13 % (*w/v*) of polyethylene glycol 8000, 15–20 % (*v/v*) of ethylene glycol, 0.03 M $MgCl_2$, 0.1 mM $ZnCl_2$, 5 mM $Na_2S_2O_4$ and 0.1 M of HEPES/NaOH buffer at pH 7.5. The drop was equilibrated against reservoir solution in the sealed well of a 96-well crystallization plate (SwissSci). Three-dimensional single crystals of vanadium nitrogenase appeared within one week and were harvested after approximately two weeks with a nylon loop for immediate flash-cooling in liquid N_2. Diffraction data were collected on beam line X06SA of the Swiss Light Source (Paul-Scherrer-Institute, Villigen, CH) using an Eiger 16M detector (Dectris). Data were indexed and integrated with XDS45 and scaled and merged with SCALA.46 Crystals of *A. vinelandii* VFe protein belonged to the triclinic space group *P*1, with unit cell dimensions of $a = 75.3$ Å, $b = 79.8$ Å and $c = 107.0$ Å, $\alpha = 84.°$, $\beta = 72.6°$ and $\gamma = 75.2°$ and contained one complete $VnfD_2K_2G_2$ heterohexamer per unit cell. For structure solution, datasets were collected to high multiplicity at and above the Fe K-edge, at wavelengths of 1.7413 Å (7120 eV, inflection)

and 1.7357 Å (7143 eV, peak), together with a high-resolution remote data set at 1.000 Å (Supplementary Table 1).

Structure solution, model building and refinement

The peak data set was used to locate a total of 30 iron sites per unit cell using SHELXD.47 An initial inspection of the sites immediately revealed a correspondence to the two copies of the 8-Fe P-cluster and 2 copies of the 7-Fe cofactor, and we consequently proceeded to site refinement and phase calculations using programs of the PHENIX suite.48 Model building into the readily interpretable electron density maps was carried out with COOT,49 and the structure was refined with REFMAC5.50 Data collection and refinement statistics are summarized in Supplementary Table 1.

Supplementary Material

Refer to Web version on PubMed Central for supplementary material.

Acknowledgements

This work was supported by the European Research Council (grant no. 310656 to O.E.) and Deutsche Forschungsgemeinschaft (RTG 1976 and PP 1927 to O.E.) and the BIOSS Centre for Biological Signaling Studies at Albert-Ludwigs-Universität Freiburg (to O.E.). We thank the beam line staff at the Swiss Light Source, Villigen, Switzerland, Günter Fritz and Anton Brausemann for their excellent assistance with data collection, and Susana Andrade for critical reading of the manuscript and helpful discussions.

References

1. Rees DC. Dinitrogen reduction by Nitrogenase - If N_2 isn't broken, It can't be fixed. Curr Opin Struct Biol. 1993; 3:921–928.
2. Rees DC, Howard JB. Nitrogenase: standing at the crossroads. Curr Opin Chem Biol. 2000; 4:559–566. [PubMed: 11006545]
3. Seefeldt LC, Hoffman BM, Dean DR. Mechanism of Mo-Dependent Nitrogenase. Annu Rev Biochem. 2009; 78:701–722. [PubMed: 19489731]
4. Howard JB, Rees DC. Structural basis of biological nitrogen fixation. Chem Rev. 1996; 96:2965–2982. [PubMed: 11848848]
5. Eady RR. Structure-function relationships of alternative nitrogenases. Chem Rev. 1996; 96:3013–3030. [PubMed: 11848850]
6. Einsle O. Nitrogenase FeMo cofactor: an atomic structure in three simple steps. J Biol Inorg Chem. 2014; 19:737–745. [PubMed: 24557709]
7. Bishop PE, Jarlenski DML, Hetherington DR. Evidence for an Alternative Nitrogen Fixation System in *Azotobacter vinelandii*. Proc Natl Acad Sci U S A. 1980; 77:7342–7346. [PubMed: 6938981]
8. Bishop PE, Hawkins ME, Eady RR. Nitrogen fixation in molybdenum-deficient continuous culture by a strain of *Azotobacter vinelandii* carrying a deletion of the structural genes for nitrogenase (*nifHDK*). Biochem J. 1986; 238:437–442. [PubMed: 3467721]
9. Bishop PE, et al. Nitrogen Fixation by *Azotobacter vinelandii* Strains Having Deletions in Structural Genes for Nitrogenase. Science. 1986; 232:92–94. [PubMed: 17774003]
10. Robson RL, et al. The Alternative Nitrogenase of *Azotobacter chroococcum* Is a Vanadium Enzyme. Nature. 1986; 322:388–390.
11. Hales BJ, Case EE, Morningstar JE, Dzeda MF, Mauterer LA. Isolation of a New Vanadium-Containing Nitrogenase from *Azotobacter vinelandii*. Biochemistry. 1986; 25:7253–7255.
12. Eady RR, Robson RL, Richardson TH, Miller RW, Hawkins M. The Vanadium Nitrogenase of *Azotobacter chroococcum* - Purification and Properties of the VFe Protein. Biochem J. 1987; 244:197–207. [PubMed: 2821997]

13. Joerger RD, et al. Nucleotide Sequences and Mutational Analysis of the Structural Genes for Nitrogenase 2 of *Azotobacter vinelandii*. J Bacteriol. 1990; 172:3400–3408. [PubMed: 2345152]
14. Eady RR. Current status of structure function relationships of vanadium nitrogenase. Coord Chem Rev. 2003; 237:23–30.
15. Lee CC, Hu YL, Ribbe MW. Unique features of the nitrogenase VFe protein from *Azotobacter vinelandii*. Proc Natl Acad Sci U S A. 2009; 106:9209–9214. [PubMed: 19478062]
16. Miller RW, Eady RR. Molybdenum and Vanadium Nitrogenases of *Azotobacter chroococcum* - Low-Temperature Favors N_2 Reduction by Vanadium Nitrogenase. Biochem J. 1988; 256:429–432. [PubMed: 3223922]
17. Lee CC, Hu YL, Ribbe MW. Vanadium Nitrogenase Reduces CO. Science. 2010; 329:642–642. [PubMed: 20689010]
18. Zhang QH, Cheng K, Kang JC, Deng WP, Wang Y. Fischer-Tropsch Catalysts for the Production of Hydrocarbon Fuels with High Selectivity. Chemsuschem. 2014; 7:1251–1264. [PubMed: 24339240]
19. Hu YL, Lee CC, Ribbe MW. Extending the Carbon Chain: Hydrocarbon Formation Catalyzed by Vanadium/Molybdenum Nitrogenases. Science. 2011; 333:753–755. [PubMed: 21817053]
20. Hu YL, Lee CC, Ribbe MW. Vanadium nitrogenase: A two-hit wonder? Dalton T. 2012; 41:1118–1127.
21. Hwang JC, Chen CH, Burris RH. Inhibition of Nitrogenase-Catalyzed Reductions. Biochim Biophys Acta. 1973; 292:256–270. [PubMed: 4705133]
22. Cameron LM, Hales BJ. Investigation of CO binding and release from Mo-nitrogenase during catalytic turnover. Biochemistry. 1998; 37:9449–9456. [PubMed: 9649328]
23. Spatzal T, Perez KA, Einsle O, Howard JB, Rees DC. Ligand binding to the FeMo-cofactor: structures of CO-bound and reactivated nitrogenase. Science. 2014; 345:1620–3. [PubMed: 25258081]
24. Spatzal T, Perez KA, Howard JB, Rees DC. Catalysis-dependent selenium incorporation and migration in the nitrogenase active site iron-molybdenum cofactor. Elife. 2015; 4:e11620. [PubMed: 26673079]
25. Sippel D, et al. Production and isolation of vanadium nitrogenase from *Azotobacter vinelandii* by molybdenum depletion. J Biol Inorg Chem. 2017; 22:161–168. [PubMed: 27928630]
26. Kim JS, Rees DC. Crystallographic Structure and Functional Implications of the Nitrogenase Molybdenum Iron Protein from *Azotobacter vinelandii*. Nature. 1992; 360:553–560. [PubMed: 25989647]
27. Zhang LM, et al. The Sixteenth Iron in the Nitrogenase MoFe Protein. Angew Chem Int Edit. 2013; 52:10529–10532.
28. Dyer DH, et al. The three-dimensional structure of the core domain of NafY from *Azotobacter vinelandii* determined at 1.8 Å resolution. J Biol Chem. 2003; 278:32150–32156. [PubMed: 12754195]
29. Homer MJ, Paustian TD, Shah VK, Roberts GP. The *nifY* Product of *Klebsiella pneumoniae* Is Associated with Apodinitrogenase and Dissociates Upon Activation with the Iron-Molybdenum Cofactor. J Bacteriol. 1993; 175:4907–4910. [PubMed: 8335644]
30. Schmid B, et al. Structure of a cofactor-deficient nitrogenase MoFe protein. Science. 2002; 296:352–356. [PubMed: 11951047]
31. Hernandez JA, et al. A Sterile alpha-Motif Domain in NafY Targets Apo-NifDK for Iron-Molybdenum Cofactor Delivery via a Tethered Domain. J Biol Chem. 2011; 286:6321–6328. [PubMed: 21156797]
32. Schindelin H, Kisker C, Sehlessman JL, Howard JB, Rees DC. Structure of ADP • AlF_4^--stabilized nitrogenase complex and its implications for signal transduction. Nature. 1997; 387:370–376. [PubMed: 9163420]
33. Tezcan FA, et al. Nitrogenase complexes: Multiple docking sites for a nucleotide switch protein. Science. 2005; 309:1377–1380. [PubMed: 16123301]
34. Peters JW, et al. Redox-dependent structural changes in the nitrogenase P-cluster. Biochemistry. 1997; 36:1181–1187. [PubMed: 9063865]

35. Tittsworth RC, Hales BJ. Oxidative titration of the nitrogenase VFe protein from *Azotobacter vinelandii*: An example of redox-gated electron flow. Biochemistry. 1996; 35:479–487. [PubMed: 8555218]
36. Rees JA, et al. The Fe-V Cofactor of Vanadium Nitrogenase Contains an Interstitial Carbon Atom. Angew Chem Int Edit. 2015; 54:13249–13252.
37. Spatzal T, et al. Evidence for Interstitial Carbon in Nitrogenase FeMo Cofactor. Science. 2011; 334:940. [PubMed: 22096190]
38. Kovacs JA, Holm RH. Assembly of Vanadium Iron Sulfur Cubane Clusters from Mononuclear and Linear Trinuclear Reactants. J Am Chem Soc. 1986; 108:340–341.
39. Varley JB, Wang Y, Chan K, Studt F, Norskov JK. Mechanistic insights into nitrogen fixation by nitrogenase enzymes. Phys Chem Chem Phys. 2015; 17:29541–29547. [PubMed: 26366854]
40. Setubal JC, et al. Genome Sequence of *Azotobacter vinelandii*, an Obligate Aerobe Specialized To Support Diverse Anaerobic Metabolic Processes. J Bacteriol. 2009; 191:4534–4545. [PubMed: 19429624]
41. Mendel RR. The Molybdenum Cofactor. J Biol Chem. 2013; 288:13165–13172. [PubMed: 23539623]
42. Lake MW, Wuebbens MM, Rajagopalan KV, Schindelin H. Mechanism of ubiquitin activation revealed by the structure of a bacterial MoeB-MoaD complex. Nature. 2001; 414:325–329. [PubMed: 11713534]
43. Wiig JA, Hu YL, Lee CC, Ribbe MW. Radical SAM-Dependent Carbon Insertion into the Nitrogenase M-Cluster. Science. 2012; 337:1672–1675. [PubMed: 23019652]
44. Lipscomb JD. Biochemistry of the Soluble Methane Monooxygenase. Annu Rev Microbiol. 1994; 48:371–399. [PubMed: 7826011]
45. Kabsch W. XDS. Acta Crystallogr D. 2010; 66:125–132. [PubMed: 20124692]
46. Evans P. Scaling and assessment of data quality. Acta Crystallogr D. 2006; 62:72–82. [PubMed: 16369096]
47. Sheldrick GM. A short history of SHELX. Acta Crystallographica Section A. 2008; 64:112–122.
48. Adams PD, et al. PHENIX: a comprehensive Python-based system for macromolecular structure solution. Acta Crystallogr D. 2010; 66:213–221. [PubMed: 20124702]
49. Emsley P, Lohkamp B, Scott WG, Cowtan K. Features and development of Coot. Acta Crystallogr D. 2010; 66:486–501. [PubMed: 20383002]
50. Murshudov GN, et al. REFMAC5 for the refinement of macromolecular crystal structures. Acta Crystallogr D. 2011; 67:355–367. [PubMed: 21460454]

Europe PMC Funders Author Manuscripts

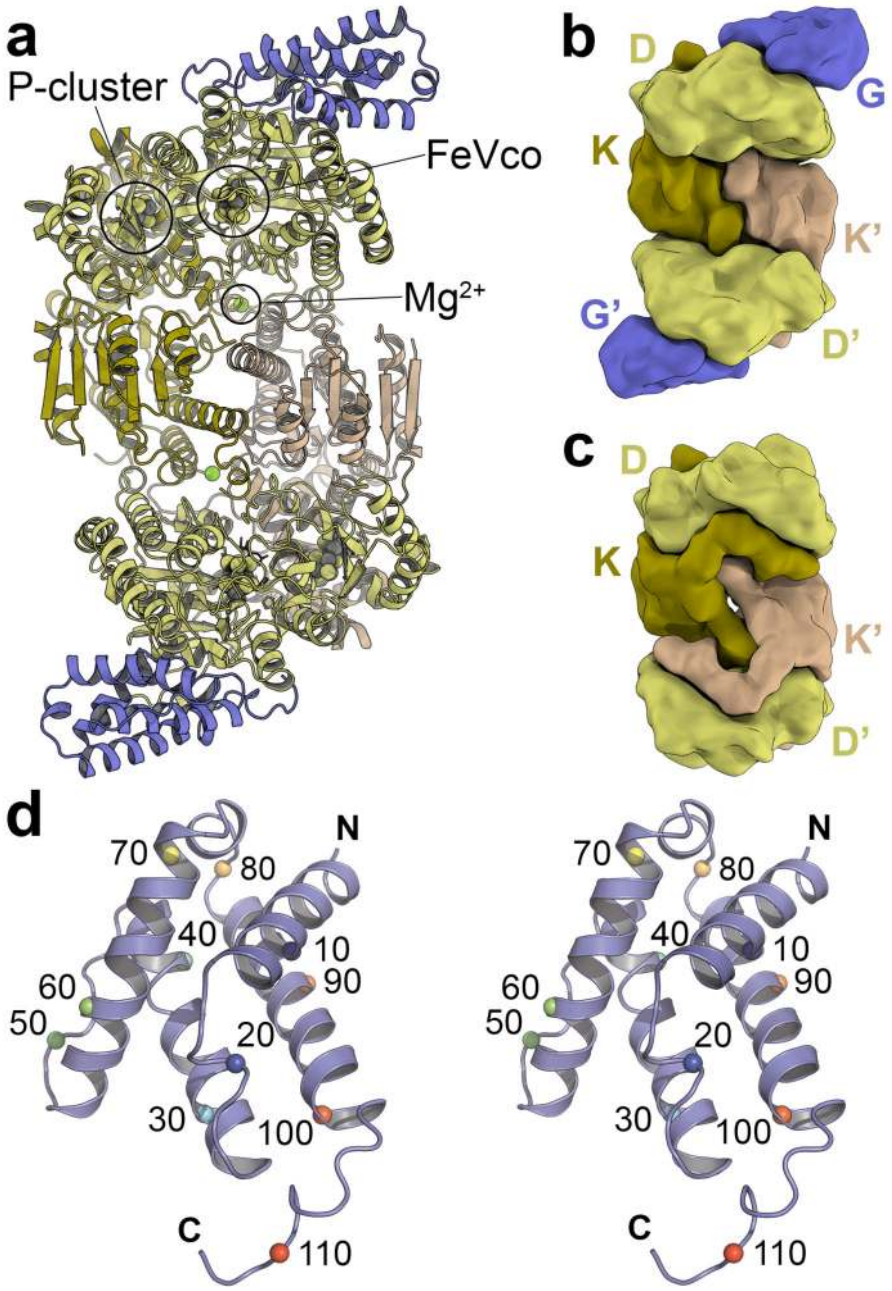

Figure 1. Structure of vanadium nitrogenase.

(**a**) Cartoon representation of the *A. vinelandii* $VnfD_2K_2G_2$ heterohexamer. Two copies of VnfG (blue) are located apically and are in exclusive contact with the adjacent VnfD subunits (yellow). The positions of the active site FeV cofactor and electron-transferring P-cluster, as well as the stabilizing Mg^{2+} cation are indicated in one monomer. (**b**) A schematic surface representation of VFe protein highlights the subunit arrangement and the positions of the VnfD, VnfK and VnfG peptides. (**c**) Molybdenum nitrogenase ($NifD_2K_2$) from the same organism shares the architecture of the core subunits, but differs markedly in aspects such as

the prominent N termini of the NifK subunits. (**d**) Stereo representation of VnfG. The subunit is a bundle of four α-helices without substantial similarities to other known structures.

Europe PMC Funders Author Manuscripts

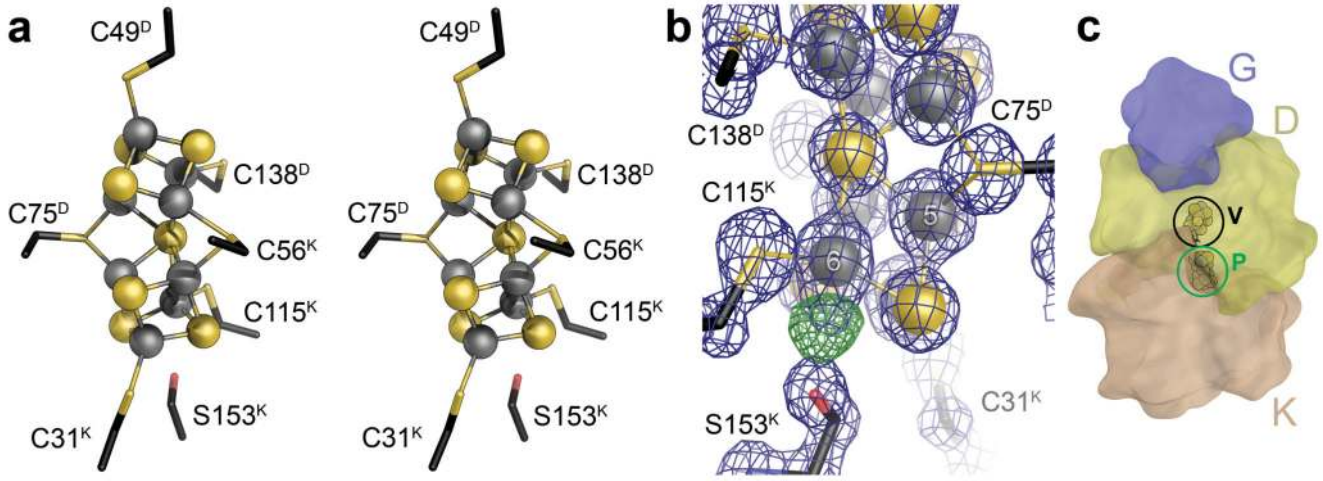

Figure 2. Electron-transferring P-cluster of vanadium nitrogenase.

(**a**) Stereo image of the [8Fe:7S] P-cluster in the reduced P^N state. Three of the six cysteine ligands to the cluster originate from VnfD, and the others from VnfK, where $S153^K$ is the conserved ligand for Fe6 in the oxidized state of the cluster. (**b**) Detail of the lower half cubane of P-cluster, highlighting Fe5 and Fe6 that in molybdenum nitrogenase relocate upon oxidation to the P^{Ox} state. The $2F_o–F_c$ electron density map (blue mesh) is contoured at the 2σ level. The green mesh shows a $F_o–F_c$ electron density map contoured at the $+6\sigma$ level, indicating the presence of a low proportion of a second conformation for Fe6. Contrary to the MoFe protein, no equivalent feature is visible at or near Fe5. The oxidized form thus likely represents a P^{1+} state as predicted by spectroscopy. (**c**) Arrangement of the subunits in a VnfDKG heterotrimer and location of the FeV cofactor (V) and the P-cluster (P). The P-cluster is centered precisely on the pseudo-twofold symmetry axis connecting VnfD and VnfK, while the VnfG subunit is in exclusive contact with VnfD.

Europe PMC Funders Author Manuscripts

Europe PMC Funders Author Manuscripts

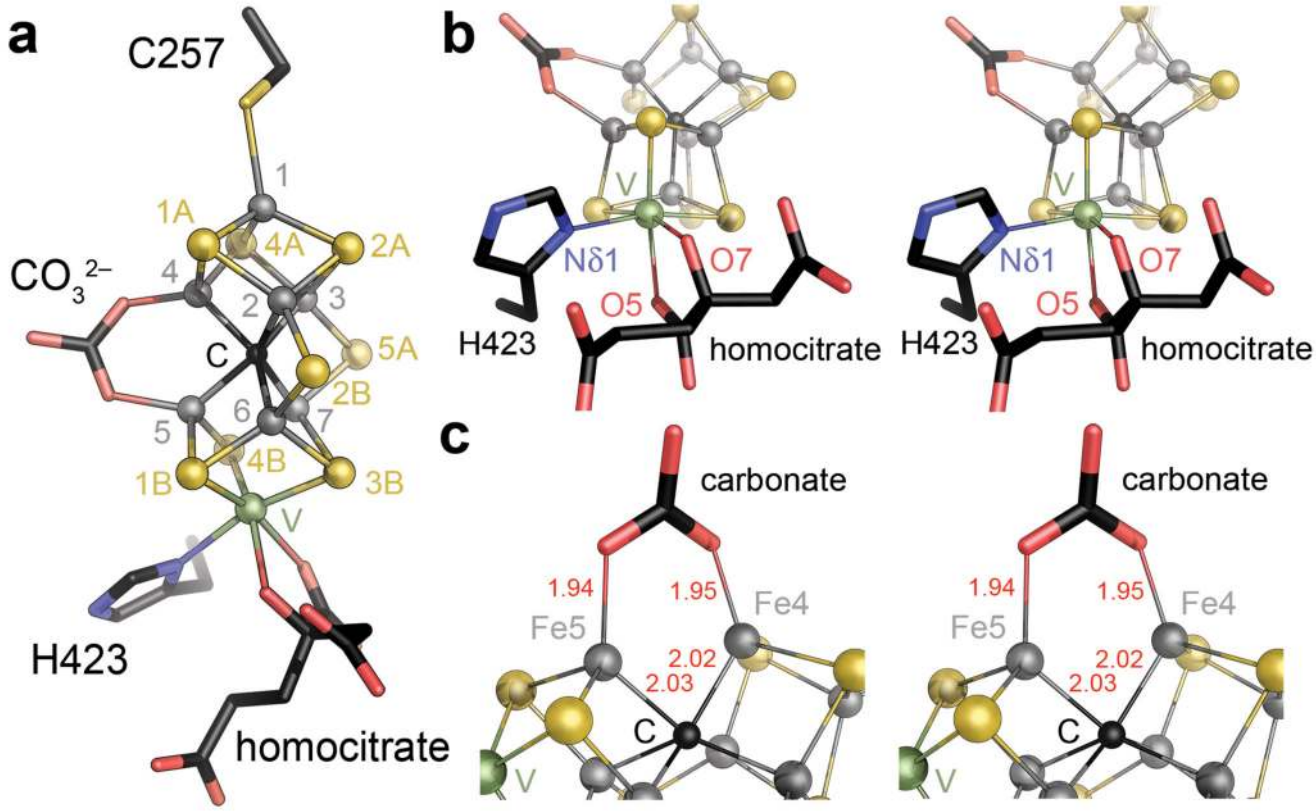

Figure 3. Structure of FeV cofactor.

(**a**) FeVco is a [V:7Fe:8S:C] cluster with a homocitrate ligand to the vanadium ion and a carbonate bridging Fe4 and Fe5. Iron ions (grey) and sulfide ions (yellow) are numbered. The cluster is coordinated to the protein *via* the amino acids C257 and H423 of VnfD. (**b**) Coordination of vanadium (stereo image). The coordinating atoms of H423 and the homocitrate moiety are labelled. (**c**) Ligation of Fe4 and Fe5 by carbonate. Average bond distances are given in Å.

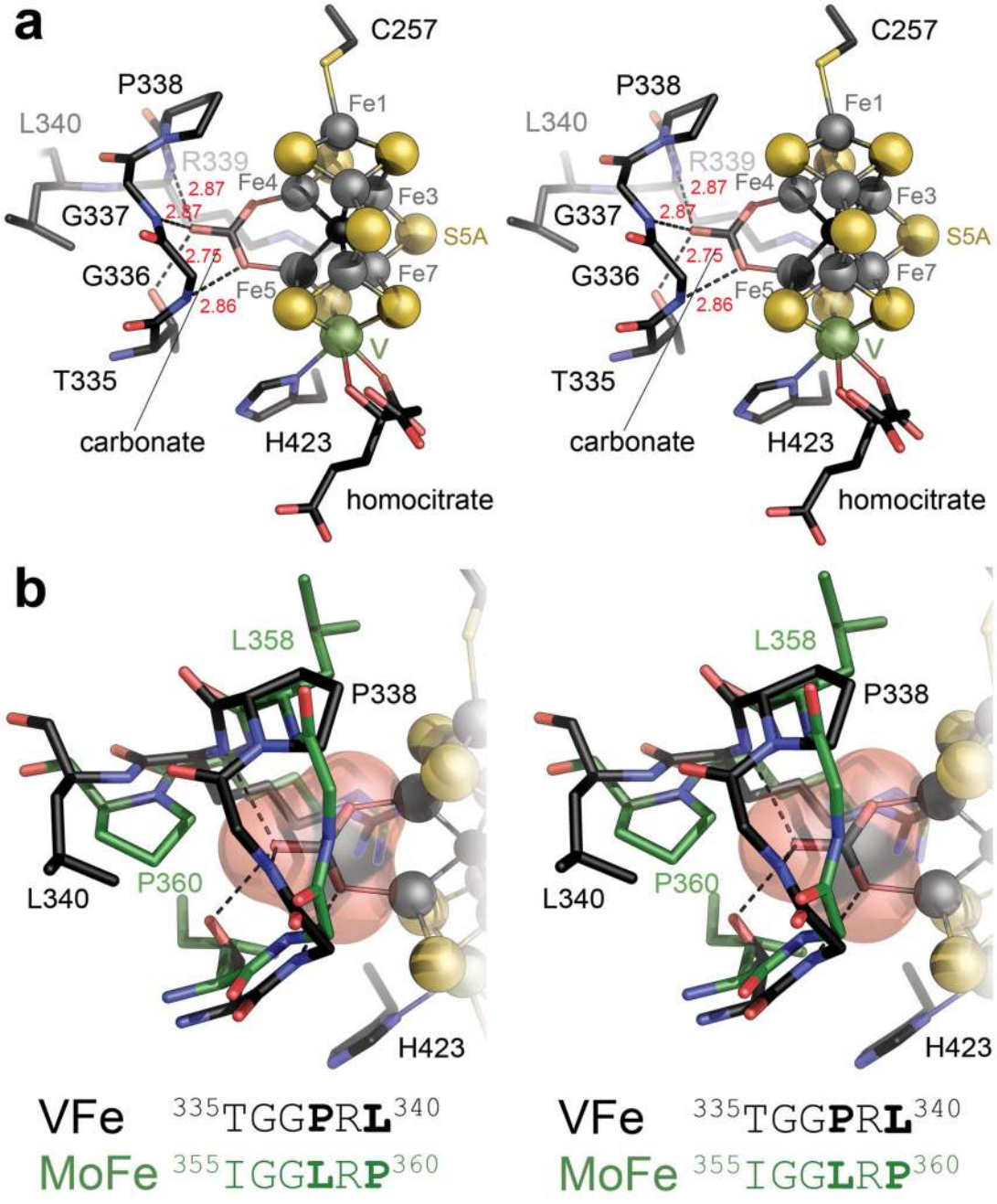

Figure 4. The carbonate ligand to FeV cofactor.

(**a**) Stereo representation of the protein environment of the carbonate ligand, CO_3^{2-}. The cluster is coordinated to the VnfD subunit of the enzyme *via* Fe1 to C257 and V to H423. (**b**) Detail of the binding pocket for the carbonate anion, coordinated by a short loop region present in both VFe protein (black) and MoFe protein (green). The swapping of a proline and a leucine in this loop leads to a slightly smaller pocket in the MoFe protein, where residue P360 would clash with the ligand.